





Point-to-multipoint beam-steering terahertz communications using a photonics-based leaky-wave transmit antenna

Jonas Tebart¹ , Joel Dittmer² , Thomas Haddad¹, Patrick Matalla², Peng Lu¹, Sebastian Randel² and Andreas Stöhr¹

Research Paper

Cite this article: Tebart J, Dittmer J, Haddad T, Matalla P, Lu P, Randel S, Stöhr A (2024) Point-to-multipoint beam-steering terahertz communications using a photonics-based leaky-wave transmit antenna. *International Journal of Microwave and Wireless Technologies*, 1–9. <https://doi.org/10.1017/S1759078724000679>

Received: 9 February 2024
Revised: 18 June 2024
Accepted: 29 June 2024

Keywords:

THz communications; Beam steering; Photonics; Leaky-wave antenna; Microwave Photonics; 6G mobile communications; Multi-beam; Wireless communications

Corresponding author: Jonas Tebart;
Email: jonas.tebart@uni-due.de

¹Department of Optoelectronics, University of Duisburg-Essen, Duisburg, Germany and ²Institute of Photonics and Quantum Electronics, Karlsruhe Institute of Technology, Karlsruhe, Germany

Abstract

We report on the successful implementation of a photonic-based beam steering approach for point-to-multipoint terahertz (THz) communications. The frequency-agile radiation properties of a THz leaky-wave antenna connected to a photodiode are utilized in the remote transmitter for generating multiple individually steerable THz beams. The approach benefits from the ultra-wide frequency tunability of optical heterodyne systems for frequency-agile THz beam steering. Moreover, the approach allows to exploit high performance and mature optical modulation techniques for generating THz beams with a high data capacity. In the THz receiver, a carrier frequency insensitive envelope THz detector based upon a single Schottky-barrier diode is used. In detail, THz communications in the 300 GHz band (WR3.4) with a maximum steering angle up to 90° is reported. Experimentally, for single steerable THz beam operation, a record high data rate of 35 Gbit/s at a wireless distance of 30 cm is achieved using two-level pulse amplitude modulation. Also, longer wireless distances up to 110 cm with 5 Gbit/s are demonstrated. Furthermore, point-to-multipoint THz communications is reported using two individually steerable THz beams carrying 10 Gbit/s and 5 Gbit/s over 70 cm and 50 cm, respectively.

Introduction

In our hyper-networked world, there is a constant need for higher transmission capacities for communication systems, which has already been discussed in literature numerous times [1, 2]. Besides the fiber infrastructure, this also applies to an increased extent to capacities in wireless communications [3, 4]. A typical method to increase the transmission capacity is to exploit extended modulation and multiplexing methods such as quadrature amplitude modulation or massive multiple-input and multiple-output systems. In addition, the allocation of new frequency bands also contributes to the increased throughput demand [5, 6]. With the introduction of new generations of mobile communications such as 6G and beyond, an expansion of the allocated spectrum to the so-called FR 2 range, which corresponds to frequencies of 24.25–52.6 GHz for FR 2-1 and 52.6–71 GHz for FR 2-2 [6, 7], is foreseen. Moreover, the use of terahertz (THz) frequencies (0.1–10 THz) for communication applications is becoming a considered approach, as enormous bandwidths are available in the frequency range around 300 GHz [8]. Initial standardization efforts were carried out in IEEE 802.15.3d as well as ITU-R F.2416-0 [9, 10]. The frequency ranges defined in these standards are largely based on the absorption properties of the atmosphere and are in the range of 252.72–321.84 GHz for the IEEE standard covering a bandwidth of about 69 GHz. The ITU also considers higher frequencies of up to 445 GHz designated for point-to-point THz links. In addition to the absorption properties of the atmosphere, the free space path loss (FSPL) also plays a significant role at such high frequencies, as it scales not only quadratically with the distance but also quadratically with the frequency [11].

Thus, FSPL is one of the reasons why mainly point-to-point THz links have been realized so far, since in such a scenario the high losses of, e.g., 122 dB at 300 GHz and 100 m transmission distance can be partially compensated by using highly directive antennas with a typical gain of >50 dBi. Examples of applications for such a transmission link are backhaul and fronthaul links in order to partially save on the deployment of fibers [12]. The research in this area of application has already shown impressive results in recent years. For example, data rates of >250 Gbit/s at 400 GHz center frequency have been demonstrated over a transmission distance of 0.5 m [13]. For transmission distances of 1 km, 56 Gbit/s have been demonstrated [14] while in [15], both, a high data rate of 200 Gbit/s and a long range of >50 m were reported.

© University of Duisburg-Essen, 2024.
Published by Cambridge University Press in association with The European Microwave Association. This is an Open Access article, distributed under the terms of the Creative Commons Attribution-ShareAlike licence (<http://creativecommons.org/licenses/by-sa/4.0/>), which permits re-use, distribution, and reproduction in any medium, provided the same Creative Commons licence is used to distribute the re-used or adapted article and the original article is properly cited.

Table 1. Summary for different beam steering concepts realized at about 300 GHz. In the case that these have also been successfully used for communication, the data rate achieved is given

| Frequency | Technology | Steering angle | Data rate | Reference |
|-----------|-------------|----------------|-----------|-----------|
| 320 GHz | SiGe BiCMOS | 24° | | [18] |
| 338 GHz | CMOS | 50° | | [19] |
| 245 GHz | Metallic | 48° | | [20] |
| 300 GHz | InP | 88° | 25 Gbit/s | [23] |
| 140 GHz | CMOS | 80° | 6 Gbit/s | [25] |
| 300 GHz | InP | 90° | 30 Gbit/s | [26] |
| 300 GHz | InP | 92° | 35 Gbit/s | This work |

However, beam steering functionality of the antenna also plays a central role for many applications. Typical examples of beam steering applications are THz hotspots or download kiosks [9, 16, 17]. The goal here is not primarily to reach long transmission distance with tens of meters, but to be able to supply users with high data rates in different spatial directions.

For the frequency range around 300 GHz – which is also used in this work – various beam steering concepts on different material platforms have already been realized. These include, e.g., phased arrays on CMOS and SiGe BiCMOS basis known from microwave technology with steering angles of up to 50° [18, 19] or meandered rectangular waveguides with radiating patches, which allow 48° steering angle [20]. On the other hand, photonic technologies are increasingly used for THz beam steering. InP-based concepts that exploit the frequency-agile properties of leaky-wave antennas (LWAs) and allow steering angles of up to 90° have been presented in [21, 22].

Nevertheless, there are very few demonstrations to date that show both, THz beam control and communications. In [23], a similar LWA to the antenna utilized in this work was implemented and 25 Gbit/s has been demonstrated at a short transmission distance of 6 cm, while in [24] an optimized transmitter architecture and digital signal processing (DSP) enabled for a data rate of 25 Gbit/s at 50 cm with the same antenna. Looking at lower frequencies, a 15 m link with 6 Gbit/s at 140 GHz and up to 80° of beam steering has been presented in [25]. An overview regarding the characteristics of the various steering concepts is given in Table 1. Additionally, the achieved data rate and the wireless distance are indicated if the steering concept was successfully used for communication.

The work in this paper is based on the system we presented in [26] for single user THz communications with up to 30 Gbit/s at 50 cm wireless transmission distance. The previous work is expanded by not only focusing on a single user at a fixed distance, but also demonstrating the transmission characteristics at different distances between transmitter and receiver (30–110 cm) in addition to the THz beam steering characteristics in a range of 30° in elevation direction. Up to 35 Gbit/s at a wireless transmission distance of 30 cm are demonstrated which is to the best of our knowledge the highest reported data rate for THz beam steering antennas. At 1.1 m, still a data rate of 5 Gbit/s is achieved. Moreover, we also exploit the multi-beam properties of the LWA and demonstrate its use in a point-to-multipoint scenario, so that two users can be served using two separated wireless communication channels with individual data simultaneously. In this case, one user is provided with 10 Gbit/s while

the other user receives a 5 Gbit/s signal at an angular separation of $\sim 15^\circ$.

On-chip LWA for THz beam steering

Antenna beam steering is an important aspect in future THz communications systems as this allows to compensate for alignment tolerances and features user mobility. Here, LWAs offer a comparatively simple approach to enable beam steering according to the applied frequency of the THz signal. It requires only a single tuning element and is capable of operating at extremely high frequencies. The following subsections first provide an introduction to the operating principles of LWAs. Then the characteristic properties such as the beam steering behavior are presented in terms of simulation as well as measurement results.

Frequency-dependent beam steering of LWAs

In general, LWAs employ a waveguide structure along which a guided electromagnetic wave propagates and controlled leakage is exploited to form radiation. For this reason, such antennas are also referred to as “traveling wave” antennas. For LWAs, the frequency dependence of the phase parameter is then typically used to realize the beam steering characteristics of the antenna as it can be seen from equation (1) for uniform LWAs [27].

$$\theta_u = \arcsin\left(\frac{\beta(\omega)}{k_0}\right) \quad (1)$$

Here θ_u is the steering angle of a uniform LWA, $\beta(\omega)$ the frequency-dependent phase parameter, and k_0 the vacuum wave number.

The introduction of periodically repeating unit-cells into the guiding structure, results in a leakage and thus a forced radiation of the wave at these interruptions by translating the non-radiating slow wave into a radiating fast wave. This also affects the phase parameter according to equation (2) as in principle an infinite number n space harmonics are created. The antenna design is then optimized to ensure an unitary fast space harmonic of $n = -1$. The incorporation of periodic structures offers a further advantage: in contrast to uniform LWAs, radiation is also possible at angles smaller than the broadside of the antenna. Thus, the steering angle θ_p that can be addressed in this way is significantly larger and can be approximated by equation (3) considering the desired first order Floquet wave ($n = -1$) at the periodic disruptions with p being the periodicity of the unit cell [28].

$$\beta_n = \beta_0 + \frac{2\pi n}{p} \quad (2)$$

$$\theta_p \approx \arcsin\left(\frac{\beta_0(\omega)}{k_0} - \frac{2\pi}{k_0 p}\right) \quad (3)$$

Moreover, this distinctive frequency dependency of the radiation direction can be used to serve a communication scenario with several users, as each frequency can be radiated at any time – i.e., also simultaneously – and thus in different spatial directions. The detailed design of the utilized LWA is discussed in the following subsection.

THz LWA design

The antenna design utilized in this work is based on periodically altered microstrip line as it can be seen in Fig. 1 and is optimized

Figure 1. Schematic LWA design based on a periodically altered microstrip line. InP is used as a substrate to allow for enhanced beam steering angles due to its high dielectric constant. A zoom-in of a unit-cell is given on the right side. It highlights the asymmetry that is used to overcome the open-stopband effect.

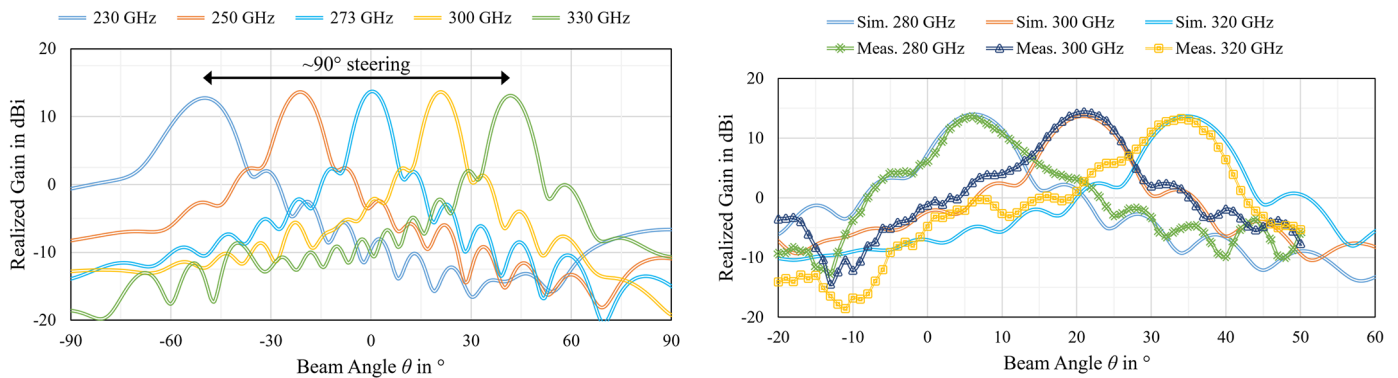
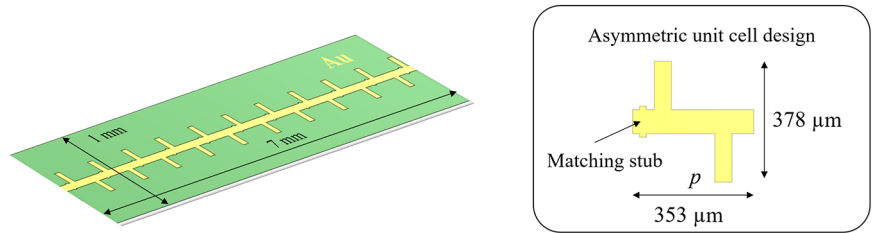


Figure 2. The simulated steering behavior of the LWA is given on the left for frequencies from 230 GHz to 330 GHz indicating a steering range of around 90° . A detailed view of the frequency and beam steering range used in the work (280–320 GHz) is shown in the graph on the right. The simulated and measured values show a good agreement and a constant peak realized gain, which is around 14 dBi for each frequency. The measurement was carried out with a spherical mm-Wave/THz antenna measurement system with 1° resolution.

for an operation within the WR3.4 band (230–330 GHz) using CST Studio Suite from Dassault Systems. Indium phosphide (InP) is used as a substrate and allows to enhance the steering range due to its high dielectric constant of $\epsilon_r = 12.4$ as the guided wavelength is affected. The antenna is fabricated on a $50 \mu\text{m}$ thin InP substrate and features 20 unit-cells, one of which is shown in more detail in the inset highlighting its asymmetry. Here, by incorporating a matching stub the symmetry is eliminated and the typically occurring open stopband effect in periodic LWAs is reduced. As reported in paper [29], a significant increase in the radiated power is realized by introducing this asymmetry, resulting in a flat gain curve compared to a design without this asymmetry.

The simulated steering behavior of the antenna for the complete WR3.4 band is depicted in Fig. 2. It shows a steering range of $\sim 90^\circ$ in the frequency range of 230–330 GHz. Due to the fact that the antenna must be contacted with a ground-signal-ground (GSG) probe, not the entire steering range can be used in practice, as reflections occur due to the probe when radiating in the backfire direction. The angular coverage considered in this work is therefore limited to angles larger than the broadside at 273 GHz. A comparison of simulated and measured realized gain for the selected region of 280–320 GHz ($\sim 5^\circ$ – 35°) is given in Fig. 2 on the right. To determine the radiation pattern a spherical mm-Wave/THz antenna measurement system was used. The measurement resolution of the system is 1° in both the elevation and azimuthal angle. In addition to a very good agreement between simulation and measurement, it also shows a flat course of the realized gain of ~ 14 dBi. It is important to mention that the LWA not only enables the emission and control of a single beam, but that all frequencies and therefore all radiation angles can be addressed at the same time. This is particularly important for the point-to-multipoint communication link.

It should be noted that only beam steering along one spatial angle (elevation) is discussed here. However, a concept for extending beam control with LWAs to the second dimension (azimuth) has already been shown in [21] by incorporating a linear phase distribution network at the input of a LWA array.

Wireless THz communications setup

The THz wireless communication transmitter used in this experiment features fiber wireless convergence and is designed to exploit the enormous bandwidths and sophisticated modulation techniques used in optical fiber communications. A block diagram of the system is shown in Fig. 3. The detailed description of the transmitter and receiver properties as well as the applied DSP chain is given in the following subsections.

Photonic transmitter for THz beam steering

As can be seen in the schematic in Fig. 3a, the waveform radiated by the LWA in the range of 300 GHz is generated by optical heterodyne mixing in an uni-travelling carrier photodiode (UTC-PD, NTT J-Band photomixer). More precisely, the photodiode generates an output signal f_{THz} which corresponds to the frequency difference of the two laser lines provided by tunable external cavity laser diodes (PurePhotonics PPCL200). Due to the enormous tunability of the lasers, it is possible to generate signals from low frequencies (MHz) up to the THz range. However, the limiting factor here is the frequency-converting component, i.e., the photodiode. In our setup, the optoelectronic conversion is optimized for the WR3.4 range, meaning the operational band of the LWA. In order to transmit a data signal in the wireless path, one of the two optical

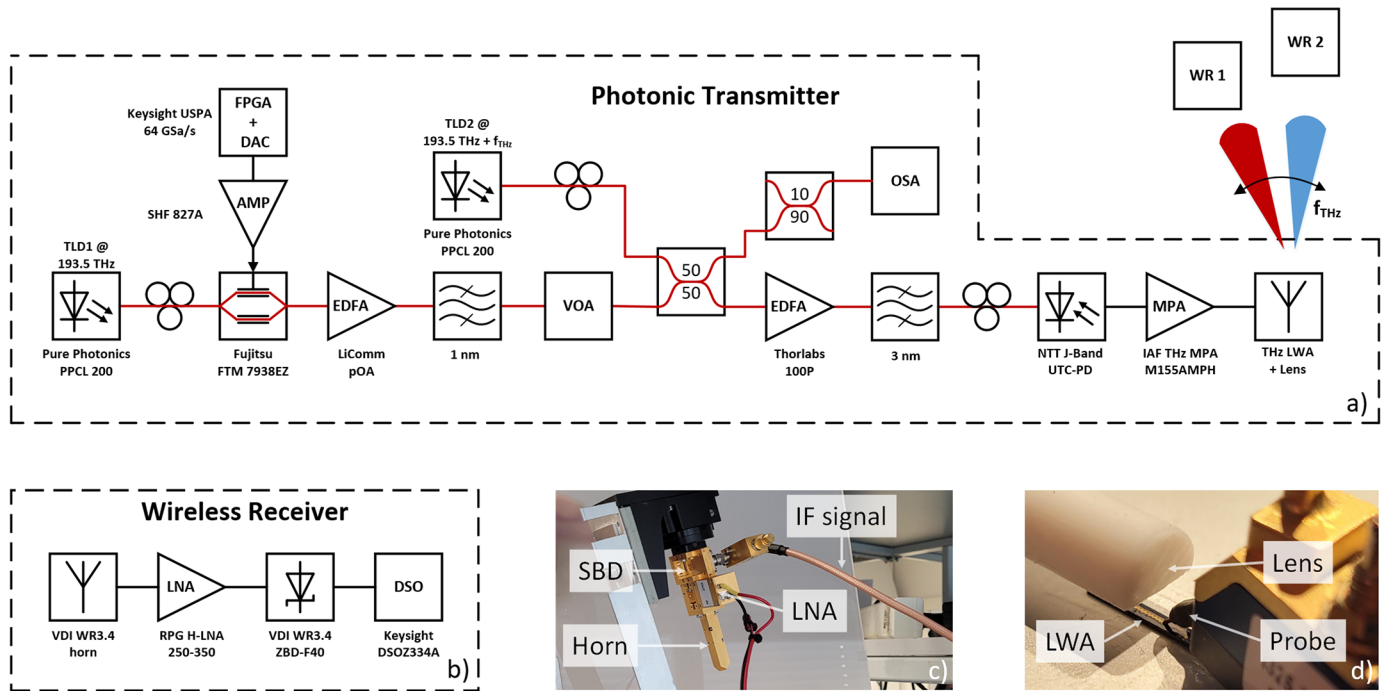


Figure 3. Schematic overview of the transmission architecture. The photonic transmitter is based on an optical heterodyne approach in combination with a LWA for beam steering and wireless communications in the frequency range around 300 GHz. Hereby, one of the optical carriers is modulated with a Mach-Zehnder modulator. The transmit data signal is generated by an FPGA in the digital domain and converted into an analog signal via a digital-to-analog converter. After optical amplification and subsequent filtering, it is down-converted into the THz range in an UTC-PD using a second tunable optical carrier that operates as a local oscillator. To enable longer wireless distances, the signal is further amplified and emitted into free space with the LWA and an additional hemispherical Teflon lens. A picture of this can be seen in (d). The steerable beam is detected by one of the wireless receivers. A detailed structure of the receiver is given in (b). After the signal is received with a horn antenna, it is further amplified by means of a power amplifier and down-converted with a Schottky-barrier diode before being digitized using a digital storage oscilloscope. A picture of the receiver is given in (c).

carriers is intensity-modulated with data using a Mach-Zehnder modulator resulting in two sidebands. The data sequence is in turn generated by a field programmable gate array (FPGA) in combination with a high-speed digital-to-analog converter (DAC) in the *Keysight Universal Signal Processing Architecture (USPA)*. To optimize the performance and quality of the signal, it is first amplified using an erbium-doped fiber amplifier (EDFA, *LiComm poA*) and then bandpass filtered to minimize the out-of-band amplified spontaneous emission (ASE) noise of the EDFA. Both optical paths are combined together using a 3 dB coupler. Here, it is ensured that the power levels are adapted to each other for optimum modulation depth. In addition, to be able to generate a sufficiently high power with the photodiode, further amplification is then required and provided by a second EDFA (*Thorlabs 100P*) with again subsequent filtering to minimize the ASE noise. The feeding power is additionally increased to about 3 dBm using a THz medium power amplifier (*Fraunhofer M155AMPH*) and fed to the antenna by a GSG probe (*FormFactor I325-T-GSG-100BT*). Taking the GSG probe losses into account, the coupled power to the antenna is about -3 dBm.

Envelope receiver for THz signal reception

At the receiver, after wireless transmission, the THz signal is detected using a comparatively simple envelope detector architecture. This comprises a horn antenna with 25 dBi gain (*VDI WR3.4 diagonal horn*) for signal reception followed by a power amplifier (*Fraunhofer M145ALNH*) with an additional gain of 24 dB at the

cost of a 10 dB noise figure. Down-conversion is then carried out by a zero-biased Schottky-barrier diode (*VDI WR3.4ZBD-F40*) which output is digitized via a digital storage oscilloscope (DSO) with 33 GHz analog bandwidth and 80 Gsa/s sampling rate (*Keysight DSA-X 93204A*). To allow for angle-dependent measurements and thus verification of the beam steering properties, the THz receiver is mounted on a goniometer. The offline DSP used to evaluate the received signal is described in the following subsection.

Digital signal processing

Transmit sequence characteristics

The pre-defined transmit sequence, which is generated in the FPGA is a two-level real-valued pulse amplitude modulated (PAM) signal. It features randomly generated symbols at rates of up to 35 Gbaud and is continuously repeated. To minimize the bandwidth of the signal, a time domain root-raised cosine filter was digitally applied. Although a low roll-off factor limits the spectrum sharply and hence would reduce spectral crosstalk between the signals of different users through the LWA, a roll-off factor of 0.8 has shown to produce the best results. The reason for this is the improved tolerance to the nonlinearity of the Schottky barrier diode (SBD) and of the LWA at higher roll-offs in the DSP.

Receiver DSP chain

For the reconstruction of the wirelessly transmitted signal, the DSP chain shown in Fig. 4 is used at the receiver side. In the first step, the received waveform is digitized using a DSO. The signal is resampled to two samples per symbol, as required by the subsequent timing



Figure 4. Digital signal processing chain to recover the transmitted waveform. After signal reception using a digital storage oscilloscope, resampling to two samples per symbol is carried out. The following feed-forward timing recovery and a subsequent blind Sato equalizer allow to reconstruct the transmit (Tx) symbols. Evaluation is then performed in terms of constellation signal to noise ratio and bit error ratio.

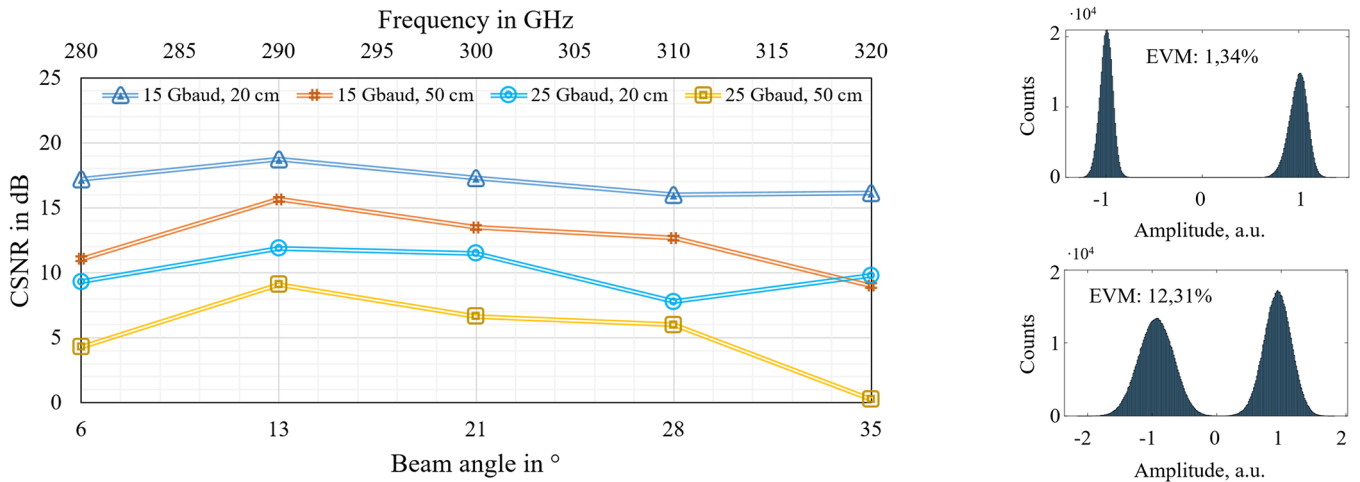


Figure 5. CSNR as a function of the beam steering angle is depicted on the left. The drop at the edges of the investigated frequency band is explainable by the frequency roll-off of the THz components and misalignment of the lens. On the top right, the histogram at 13° steering angle (290 GHz) and a symbol rate of 15 Gbaud at 20 cm wireless distance is given. In contrast, the histogram down right corresponds to 25 Gbaud and 50 cm at the same steering angle.

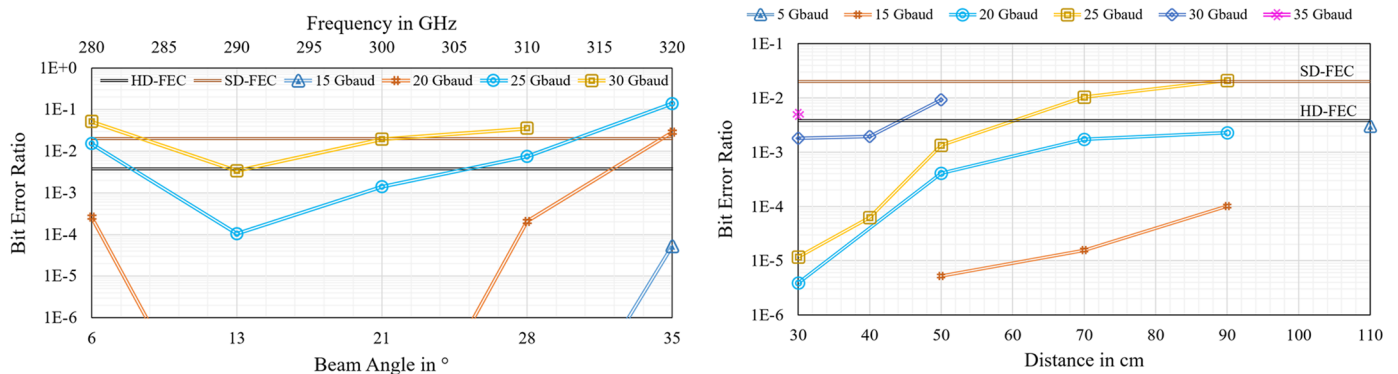


Figure 6. On the left, the BER is given as a function of the beam steering angle and frequency at a wireless distance of 50 cm and symbol rates of 15–30 Gbaud. Transmitting PAM2 and taking the HD-FEC limit into account, up to 30 Gbit/s have been transmitted error-free at 290 GHz. On the right, the BER is shown as a function of wireless distance and fixed frequency of 280 GHz for different symbol rates. A maximum data rate of 35 Gbit/s was achieved at 30 cm with SD-FEC limit. At the highest distance examined (110 cm), the maximum data rate is 5 Gbit/s.

recovery. Here, we apply a feed-forward timing recovery according to the algorithm proposed by Barton and Al-Jalili [30, 31].

The next step in recovering the signal involves the application of a fully blind equalizer. This allows mitigation of channel impairments, e.g., transceiver bandwidth limitations and channel effects. The approach is based on a minimization of the cost function, which describes the distance between the expected and the actual symbol value, as proposed by Sato [32]. The necessary filter coefficients are then adapted blindly using the stochastic gradient descent method.

This brings advantages in terms of the transmitted net data rate compared to preamble-based equalizers, which determine the distortion of a channel by transmitting a known symbol sequence. In addition, down-sampling by a factor of two is performed after the Sato equalizer and, as a result, the transmitted symbols are

recovered at the end of the DSP chain. An evaluation of the recovered signal is then carried out on the basis of constellation signal to noise ratio (CSNR) and bit error ratio (BER) to provide an indication of the transmission quality. The results are presented in the following subsections.

Measurement results for single and multipoint communications

To validate the beam steering properties of the THz communication system, measurements were first carried out for a single user. The results of this are summarized in subsection “THz beam steering communications for single users.” Then, the multi-user functionality is examined in more detail in subsection “Simultaneous point-to-multipoint THz communications.”

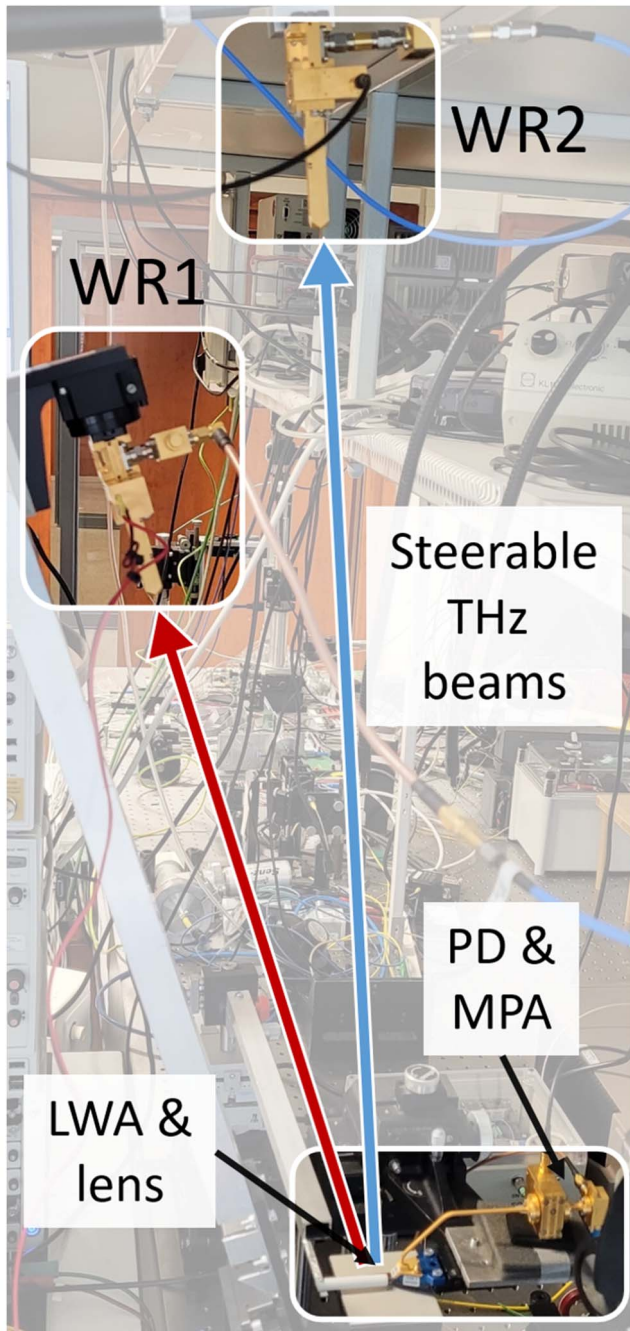


Figure 7. The image shows the point-to-multipoint setup with two users that can simultaneously receive individual data at different locations.

THz beam steering communications for single users

In the first step, to obtain information about the transmission quality in different spatial directions, the received signal was evaluated on the basis of the CSNR for two distances (20 cm and 50 cm) and symbol rates (15 Gbaud and 25 Gbaud) at different THz center frequencies. The results are illustrated in Fig. 5. A rather flat CSNR characteristic can be seen, particularly in the 290–310 GHz range (13° – 28°), which confirms the expectations from the simulations with regard to the linear antenna gain over this frequency range.

However, when approaching the edges of the steering range considered here, a stronger drop in the CSNR can be observed,

Table 2. Summary of the main transmission properties for the point-to-multipoint experiment indicating the receiver locations and the maximum achievable HD-FEC compliant data rates

| | Wireless receiver 1 | Wireless receiver 2 |
|------------------------|----------------------|----------------------|
| Wireless distance | 50 cm | 70 cm |
| Beam steering angle | 17° | 6° |
| Transmission frequency | 300 GHz | 280 GHz |
| Baud rate | 5 Gbaud | 10 Gbaud |
| Modulation | PAM2 | PAM2 |
| Bit error rate | 2.2×10^{-3} | 3.4×10^{-3} |

especially at higher distances and symbol rates. In our scenario, this can be explained partly by the frequency roll-off of the THz components (photodiode, Tx and Rx amplifier) and partly by a slight misalignment between Teflon lens and LWA, which leads to a broadening of the beam. In addition, the frequency-dependent beam steering behavior of the LWA must also be taken into account when considering larger distances, as this is becoming more significant. From the steering parameter ($0.725^{\circ}/\text{GHz}$) and the 3 dB beamwidth ($\sim 10^{\circ}$), it can be seen that the signal bandwidth that is detectable by a highly directive receiver must be reduced in this scenario.

The histogram after the linear equalizer and down-sampling for two exemplary measurements are given in the right part of Fig. 5. The upper histogram is measured at 15 Gbaud and 290 GHz, i.e., an angle of 13° , with a wireless distance of 20 cm. Here, the two signal levels are nicely separated leading to an error-free transmission. In contrast, a noticeable broadening of the symbol levels can be seen in the figure below. This corresponds to a measurement at the same angle but now with a 25 Gbaud symbol rate and a distance of 50 cm. In both cases, however, error-free transmission is still possible considering a hard-decision forward error correction (HD-FEC) limit of 3.8×10^{-3} , as it is further indicated by Fig. 6 on the left. Here, we generally aim to analyze the BER behavior as a function of beam steering for different symbol rates at a fixed distance of 50 cm. As already expected from the consideration of the CSNR, higher BERs can be observed especially at the highest transmit frequency (320 GHz), so that the maximum achievable data rate here is 15 Gbit/s using PAM2 modulation. However, if the focus is set to the core frequency range of 280–310 GHz ($>20^{\circ}$ steering coverage), data rates of 25 Gbit/s are supported considering the soft-decision forward error correction (SD-FEC) limit of 2×10^{-2} . The best transmission characteristics are recorded with 30 Gbit/s (HD-FEC compliant) at 290 GHz.

In addition to a demonstration of the beam steering behavior, measurements were carried out at a fixed angle of 6° (280 GHz) and variable distance in the range of 30–110 cm. The results are shown in Fig. 6 on the right. As can be seen from this, the maximum error-free transmitted data rate is 35 Gbit/s at a distance of 30 cm, assuming SD-FEC as the limit, which to the best of our knowledge is the highest reported value for THz beam steering antennas.

Simultaneous point-to-multipoint THz communications

Besides transmission to a single user, the multi-beam property of the LWA have been exploited for addressing two users simultaneously. The transmission experiment is also based on the communications architecture introduced in section “Wireless

THz communications setup.” However, a slight change was made to the baseband signal generation. Instead of the previously used FPGA and DAC, an arbitrary waveform generator (AWG, Keysight M8194A) with a higher baseband bandwidth of 50 GHz was used here. In this way, it is possible to distribute individual user data over a wider spectrum already in the digital domain. With regard to the LWA, this offers the possibility of different data being transmitted in a wider angular coverage. Compared to the approach of using an additional laser that acts as a second local oscillator (LO) at a slightly offset wavelength and thus different steering angle, as shown in paper [23], the system utilized here offers the possibility that individual data can be transmitted to different users simultaneously. Hereby, the angle at which the signal is radiated is set via the digital frequency up-conversion of the signal. This means that if the angle to the receiver is known, the frequency shift – and thus the radiation angle – can be adjusted in the digital domain so that the particular user is provided with individual data as long as they do not obscure each other. As there is no inherent tracking functionality in the presented system, the position of the receivers can be varied, but manual adjustment of the transmission signal is required.

A picture of the setup with two wireless receivers is depicted in Fig. 7 and Table 2 gives an overview on the main transmission properties. As can be seen, the receivers are located at a wireless distance of 50 cm and 70 cm, respectively and angles of 17° and 6°. The corresponding center frequencies are 300 GHz and 280 GHz. Once again, it should be noted that the 20 GHz offset between the two data signals was already generated in the transmission sequence in the digital domain.

Overall, simultaneous data transmission of 5 Gbit/s for wireless receiver 1 (WR1) and 10 Gbit/s for wireless receiver 2 (WR2) was demonstrated while complying with the HD-FEC limit.

In the current system, both the transmitting and the receiving side influence the maximum number of supported users. From the transmitting side, the relatively high roll-off factor plays a particular role as neighboring receivers are affected by interference. On the other hand, the transmitting side is also influenced by the receiver architecture. By using an SBD receiver, it is necessary that the transmit waveform contains an additional carrier for down-conversion. This means that the maximum power level in each data signal is reduced. One way to improve this would be to implement a heterodyne receiver in which the required carrier for down-conversion is generated at the receiver. However, as shown in [15], the use of an intradyne receiver is significantly better in terms system performance compared to a heterodyne receiver, which is why this approach will be pursued in upcoming systems. In [23] it was shown with a similar LWA that a 1 GHz guard band is sufficient for the separation of two users. Under this assumption, the concept presented here can be used to generate seven simultaneous beams in the 280–320 GHz frequency range, each with a bandwidth of 5 GHz, which would correspond to a total throughput of 35 Gbit/s.

Conclusion

We have successfully demonstrated point-to-multipoint THz communications in the 300 GHz band utilizing the frequency-agile beam steering properties of a THz LWA connected to a UTC-PD. The planar LWA antenna, which is based upon a periodically alternated microstrip line, supports a maximum beam steering angle of 90° in the frequency range between 230 and 330 GHz. The direct photonic-wireless convergence approach is based on optical heterodyne THz beam generation by mixing two optical carriers in

a high-speed UTC-PD. By tuning the frequency of one of the lasers, the transmit angle of the generated THz beam is changed. This is a significantly easier steering approach as compared to phased arrays which require to control the THz phase or delay at each antenna element. In the THz receiver, a carrier frequency insensitive envelope detector based upon a single SBD is used. Offline DSP is carried out based on a fully blind Sato equalizer.

Experimentally, a maximum data rate for single steerable THz beam operation of 35 Gbit/s is successfully transmitted over a wireless distance of 30 cm with a BER below SD-FEC limit, which, to the best of our knowledge, is the highest reported data rate for THz beam steering antennas. Within a steering angle of 22°, a single user can be supplied with 25 Gbit/s at a wireless distance of 50 cm.

Moreover, simultaneous point-to-multipoint THz communication is experimentally demonstrated using two individually steerable beams and two users located at different beam angles and wireless distances. This is achieved by utilizing a multicarrier baseband signal which is basically converted by the photonics-based THz transmitter into two individually steerable THz beams carrying independent data. In detail, one user located at a beam angle of 6° at a wireless distance of 70 cm receives a PAM2 modulated THz beam with 10 Gbit/s. Simultaneously, the second user located at 17° at a wireless distance of 50 cm is supported with 5 Gbit/s.

The presented approach utilizes a multi-carrier baseband signal to support multiple individually THz beams. For each beam, a PAM2 double-sideband signal with carrier is used. This limits the maximum number of beams that can be supported simultaneously, and it also limits the maximum data rate per beam. The use of complex modulated single sideband signals without carriers in combination with an improved receiver architecture based on an intradyne THz receiver should significantly increase the transmission capacity. Due to the higher spectral efficiency, at least a doubling is expected at the same transmission distance. In addition, there is potential to extend the wireless transmission distance. In the simplest case, this can be realized by implementing an LWA array and thus increasing the antenna gain due to the array factor. An array arrangement also offers the possibility of extending beam steering in azimuth direction by controlling the phase of each individual antenna element. In this context, the integration of the photodiodes with the antennas is also being encouraged in order to avoid interface losses through the use of probes.

Application scenarios for the point-to-multipoint communication system include THz hotspots for download kiosks or inter- and intra-rack communications.

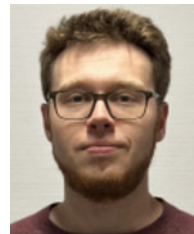
Funding statement. This work is supported by the German Federal Ministry of Education within the projects 6GEM (A.S., grant number 16KISK039) and Open6GHub (S.R., grant number 16KISK010 and A.S., grant number 16KISK017), the German Research Foundation within the collaborative research center Marie CRC/TRR 196 (A.S., grant number 287022738) as well as European Union's Horizon 2020 Research and Innovation Program under Marie Skłodowska-Curie project, TERAOPTICS (A.S., grant number 956857).

Competing interests. The authors report no conflict of interest.

References

1. CISCO (2017) Cisco Visual Networking Index (VNI) Update Global Mobile Data Traffic Forecast. White Paper.
2. Agrell E, Karlsson M, Chraplyvy A R, Richardson D J, Krummrich P M, Winzer P, Roberts K, Fischer J K, Savory S J, Eggleton B J, Secondini M, Kschischang F R, Lord A, Prat J, Tomkos I, Bowers J E, Srinivasan S, Brandt-Pearce M and Gisin N (2016) Roadmap of optical communications. *Journal of Optics* 18, 063002.

3. Nagatsuma T, Ducournau G and Renaud C (2016) Advances in terahertz communications accelerated by photonics. *Nature Photonics* **10**, 371–379.
4. Koenig S, Lopez-Diaz D, Antes J, Boes F, Henneberger R, Leuther A, Tessmann A, Schmogrow R, Hillerkuss D, Palmer R, Zwick T, Koos C, Freude W, Ambacher O, Leuthold J and Kallfass I (2013) Wireless sub-THz communication system with high data rate. *Nature Photonics* **7**, 977–981.
5. Guo S, Zhang H, Zhang P, Zhao P, Wang L and Alouini M-S (2019) Generalized beamspace modulation using multiplexing: A breakthrough in mmWave MIMO. *IEEE Journal on Selected Areas in Communications* **37**(9), 2014–2028.
6. Chen W, Montojo J, Lee J, Shafi M and Kim Y (2022) The standardization of 5G-advanced in 3GPP. *IEEE Communications Magazine* **60**(11), 98–104.
7. Rohde & Schwarz (2020) 5G Evolution – On the path to 6G, Expanding the frontiers of wireless communications. White Paper.
8. Chowdhury M, Shahjalal M, Ahmed S and Jang YM (2020) 6G wireless communication systems: Applications, requirements, technologies, challenges, and research directions. *IEEE Open Journal of the Communications Society* **1**, 957–975.
9. Petrov V, Kürner T and Hosako I (2020) IEEE 802.15.3d: First standardization efforts for sub-terahertz band communications toward 6G. *IEEE Communications Magazine* **58**(11), 28–33.
10. ITU-R. Report ITU-R F.2416 Technical and operational characteristics and applications of the point-to-point fixed service applications operating in the frequency band 275–450 GHz. <https://www.itu.int/pub/R-REP-F.2416>.
11. Balanis CA (2008) *Modern Antenna Handbook*. Hoboken, NJ: Wiley.
12. Singh R and Sicker D (2019) Beyond 5G: THz spectrum futures and implications for wireless communication. In *Proceedings 30th European Conference of the International Telecommunication Society (ITS)*, June 16–19, 2019. <https://www.econstor.eu/bitstream/10419/205213/1/Singh-Sicker.pdf>.
13. Pang X, Jia S, Ozolins O, Yu X, Hu H, Marcon L, Guan P, Da Ros F, Popov S, Jacobsen G, Galili M, Morioka T, Zibar D and Oxenløwe L K (2016) 260 Gbit/s photonic-wireless link in the THz band. In *2016 IEEE Photonics Conference (IPC)*, Waikoloa, HI, USA, 1–2.
14. Castro C, Elschner R, Merkle T, Schubert C and Freund R (2020) Long-range high-speed THz-wireless transmission in the 300 GHz band. In *2020 Third International Workshop on Mobile Terahertz Systems (IWMTS)*, Essen, Germany, 1–4.
15. J. Dittmer J, Füllner C, Stöhr A and Randel S (2023) 200 Gbit/s wireless THz transmission over 52m using optoelectronic signal generation. In *2023 53rd European Microwave Conference (EuMC)*, Berlin, Germany, 134–137.
16. Ducournau G, Pavanello F, Beck A, Tohme L, Blin S, Nouvel P, Peytavit E, Zaknoute M, Szzriftgiser P and Lampin J F (2014) High-definition television transmission at 600 GHz combining THz photonics hotspot and high-sensitivity heterodyne receiver. *Electronics Letters* **50**(5), 413–415.
17. Song H-J, Hamada H and Yaita M (2018) Prototype of KIOSK data downloading system at 300 GHz: Design, technical feasibility, and results. *IEEE Communications Magazine* **56**(6), 130–136.
18. Deng X-D, Li Y, Li J, Liu C, Wu W and Xiong Y-Z (2015) A 320-GHz 1×4 fully integrated phased array transmitter using 0.13- μm SiGe BiCMOS technology. *IEEE Transactions on Terahertz Science and Technology* **5**(6), 930–940.
19. Tousei Y and Afshari E (2015) A high-power and scalable 2-D phased array for terahertz CMOS integrated systems. *IEEE Journal of Solid-State Circuits* **50**(2), 597–609.
20. Sarabandi K, Jam A, Vahidpour M and East J (2018) A novel frequency beam-steering antenna array for submillimeter-wave applications. *IEEE Transactions on Terahertz Science and Technology* **8**(6), 654–665.
21. Haddad T, Biurrun-Quel C, Lu P, Tebart J, Sievert B, Makhlof S, Grzeslo M, Teniente J, Del-Río C and Stöhr A (2022) Photonic-assisted 2-D terahertz beam steering enabled by a LWA array monolithically integrated with a BFN. *Optics Express* **30**, 38596.
22. Lu P, Haddad T, Tebart J, Roeloffzen C and Stöhr A (2022) Photonic integrated circuit for optical phase control of 1 × 4 terahertz phased arrays. *Photonics* **9**(12), 902.
23. Lu P, Haddad T, Tebart J, Steeg M, Sievert B, Lackmann J, Rennings A and Stöhr A (2021) Mobile THz communications using photonic assisted beam steering leaky-wave antennas. *Optics Express* **29**, 21629.
24. Tebart J, Lu P, Haddad T, Iwamatsu S and Stöhr A (2023) Prospects and technologies for mobile terahertz 6G communications. In *Optical Fiber Communications Conference and Exhibition (OFC)*, 1–3.
25. Abu-Surra S, Choi W, Choi S, Seok E, Kim D, Sharma N, Advani S, Loseu V, Bae K, Na I, Farid A A, Rodwell M J W, Xu G and Zhang J (2021) End-to-end 140 GHz wireless link demonstration with fully-digital beam-formed system. In *2021 IEEE International Conference on Communications Workshops (ICC Workshops)*, Montreal, QC, Canada, 1–6.
26. J. Tebart J, Haddad T, Lu P, Randel S and Stöhr A (2023) Mobile 6G communications at THz frequencies enabled by leaky-wave antenna beam steering. In *2023 53rd European Microwave Conference (EuMC)*, Berlin, Germany, 142–145.
27. Chen ZN, Liu D, Nakano H, Qing X and Zwick T (2016) *Handbook of Antenna Technologies*. Berlin: Springer Publishing Company.
28. Jackson DR, Caloz C and Itoh T (2012) Leaky-wave antennas. *Proceedings of the IEEE* **100**(7), 2194–2206.
29. Haddad T, Biurrun-Quel C, Lu P, Kaya H, Mohammad I and Stöhr A (2023) Suppressing open stopband for terahertz periodic microstrip leaky-wave antennas. In *2023 17th European Conference on Antennas and Propagation (EuCAP)*, Florence, Italy, 1–5.
30. Barton SK and Al-Jalili YO (1992) A symbol timing recovery scheme based on spectral redundancy. In *IEEE Colloquium on Advanced Modulation and Coding Techniques for Satellite Communications*.
31. Matalla P, Mahmud MS, Füllner C, Freude W and Randel S (2021) Hardware comparison of feed-forward clock recovery algorithms for optical communications. In *2021 Optical Fiber Communications Conference and Exhibition (OFC)*, San Francisco, CA, USA, 1–3.
32. Sato Y (1975) A method of self-recovering equalization for multilevel amplitude-modulation systems. *IEEE Transactions on Communications* **23**(6), 679–682.



Jonas Tebart received the B.Sc. and M.Sc. degrees in electrical engineering and information technology from the University of Duisburg-Essen, Duisburg, Germany, in 2016 and 2019, respectively, where he is currently pursuing the Ph.D. degree under the supervision of Prof. Andreas Stöhr. After his studies with focus on microelectronics and optoelectronics, he joined the Department of Optoelectronics, University of Duisburg-Essen, as a Research Assistant. His research interests include radio-over-fiber (RoF) techniques, millimeter-wave (mm-wave) and THz communications, 5G, B5G and 6G mobile networks, photonic radars, as well as mm-wave beam-steering antennas.



Joel Dittmer was born in Karlsruhe, Germany, in 1995. He received the B.Sc. and M.Sc. degrees in electrical engineering from the Karlsruhe Institute of Technology, Karlsruhe, Germany, in 2020 and 2022, respectively. He joined the Institute of Photonics and Quantum Electronics (IPQ) at the Karlsruhe Institute of technology in 2023, where he started as a research assistant in the field of optoelectronic and electronic generated terahertz signals for wireless communications. His research interests include THz system design, THz package design, and high data rate digital signal processing.



Thomas Haddad (Graduate Student Member, IEEE) received the M.Sc. degree in embedded systems from the University of Duisburg-Essen, Duisburg, Germany, in 2019. He joined the Department of Optoelectronics at the University of Duisburg-Essen in 2020, where he is working toward the Ph.D. degree and conducting scientific research in MARIE CRC/TRR 196 project under the supervision of Prof. Andreas Stöhr. His research interests include the design and fabrication

technologies of integrated photonic chips (PICs) with 2D THz beam steering for THz imaging and THz communications.



Patrick Matalla received the B.Sc. and M.Sc. degrees in electrical engineering from the Karlsruhe Institute of Technology, Karlsruhe, Germany, in 2018 and 2020, respectively. He joined the Institute of Photonics and Quantum Electronics (IPQ) at the Karlsruhe Institute of Technology in 2020, where he is currently working toward his Ph.D. degree. His research interests include optical communication systems and the hardware implementation of digital signal

processing algorithms on field-programmable gate arrays (FPGAs).



Peng Lu was born in Tianjin, China. He received the B.Sc. and M.Sc. degrees in nanoengineering/nano-optoelectronics from the University of Duisburg-Essen, Duisburg, Germany, in 2014 and 2016, respectively. Since 2017, he has been a Member of the Department of Optoelectronics, Center for Semiconductor Technology and Optoelectronics (ZHO), and a Research Associate with the University of Duisburg-Essen. His current research interests include photonic integrated chips (PICs) for terahertz beam forming, terahertz

leaky-wave antenna, and 3D hybrid integration of III-V-Si platforms.



Sebastian Randel (Senior Member, IEEE) received the Dr.-Ing. degree for his work on high speed optical-time-division-multiplexed transmission systems from Technische Universität Berlin, Berlin, Germany, in 2005. He is currently a full Professor with the Karlsruhe Institute of Technology, Karlsruhe, Germany, where he is co-heading the Institute of Photonics and Quantum Electronics. From 2005 to 2010, he was a Research Scientist with Siemens Corporate

Technology, Munich, Germany, where he led research and standardization activities in the fields of polymer-optical-fiber communications, visible light communications, and optical access networks. From 2010 to 2016, he was a Member of Technical Staff with Bell Laboratories, Holmdel, NJ, USA. His research focuses on the design and the implementation of power-efficient DSP algorithms for high-performance coherent optical transceivers.



Andreas Stöhr (Senior Member, IEEE) received the Dipl.-Ing. and Dr.-Ing. degrees in electrical engineering from Gerhard-Mercator University, Duisburg, Germany, in 1991 and 1997, respectively. From 1996 to 2013, he was a Research Scientist at the University of Duisburg-Essen (UDE), Duisburg. Between 1998 and 1999, he joined the Communications Research Laboratory, Tokyo, Japan. He was with France Telecom Orange Labs, France, in 2009, and Corning, in 2015. Since

2011, he has been a Professor and the Head of the Center for Semiconductor Technology and Optoelectronics, Optoelectronics Department, UDE. He has authored or coauthored more than 200 papers in journals and conferences. His research interests include III/V integrated microwave photonics and RF photonic integration for millimeter-wave and THz communications, measurement systems, and sensing applications. He is Senior Member of the IEEE Photonics and MTT Society, committee member and the chair of a number of international conferences, and the Guest Editor of IEEE/OSA.